Original Research Article

Kinetics of Enhancer-monomer for Corneal Cross-linking: Proposed Model for a two-monomer system

ABSTRACT

Aims: To derive kinetic equations and analytic formulas for efficacy enhancement of corneal collagen crosslinking (CXL) in a 2-monomer system.
Study Design: modeling the kinetics of CXL
Place and Duration of Study: Taipei, Taiwan, between between January 2019 to June, 2019.
Methodology: Coupled rate equations are derived for two monomers system, [A] for the corneal collagen substrate, and [B] for an additive enhancer, having 3 crosslinking pathways: two radical-mediated (or electron transfer) pathways, and one oxygen-mediated (or energy transfer) pathway. The reactive intermediates [R] and [S] which could interact with oxygen [A], [B], or bimolecular termination. For a type-II (or oxygen-mediated) process, [T] interacts with $[O_2]$ to form a singlet oxygen $[O_1]$ which could interact with [A], [B], or relaxed to $[O_2]$. Rate equations, based on lifetime of photosensitizer triplet-state and oxygen singlet-state, are used to analyze the measured results in a rose-Bengal system with an enhancer-monomer.

Results: Additive enhancer-monomer of arginine added to a rose Bengal photosensitizer may enhance the production of free radicals under a green-light CXL. D_2O may extends the lifetime of oxygen singlet state and thus improve the efficacy. Our formulas predicted features are consistent with the measured results.

Conclusion: Efficacy may be improved by enhancer-monomer or extended lifetime of photosensitizer triplet-state or oxygen singlet state.

Keywords: Corneal crosslinking; corneal keratoconus; efficacy; kinetic modeling; oxygen; riboflavin; rose Bengal, ultraviolet light;.

1. INTRODUCTION

Photochemical kinetics of corneal collagen crosslinking (CXL) has been extensively studied using UVA light and riboflavin (RF) as the photosensitizer [1-6]. Much less efforts have been reported using green-light and rose Bengal (RB) as the photosensitizer [7-9]. Comparison of animal studies of corneal biomechanical properties after in vivo and ex vivo CXL using rose-Bengal–green light (RGX) or riboflavin-UVA (UVX) was reported by Bekesi et al [8] that the CXL anterior part was 100 and 143 to 188 um for RGX and UVX, respectively. We have previously considered a one-monomer system for the UVX, in which type-I is the predominant process [6,10,11]. In contrast, RGX is predominated by an oxygen-mediated type-II process, where the single-monomer radical induced type-I conversion is not very efficient [7]. Therefore, additive enhancer-monomer was proposed by Wertheimer et al [7] for improved overall (type-I plus type-II) efficacy. For type-I predominant UVX, single-monomer has sufficient efficacy and there is no need to add another enhancer-monomer. A 2-monomer system offers an enhanced enhanced efficacy, however, it is limited by the available enhancers, and more difficult to control the precise concentrations and might take longer preoperative time for sufficient diffusion of the two monomers. In comparison, a single-monomer system is simpler and clinically easier to administrate its concentration.

This article will present a 2-monomer model system, for the first time, to analyze the measured results of Wertheimer et al [7], where efficacy may be enhanced by an enhancer-monomer or increase the lifetime of photosensitizer triplet-state and oxygen singlet-state.

2. MATERIALS AND METHODS

As shown by Fig. 1, a two-monomer system is proposed: [A] for the corneal collagen substrate and [B] as an additive enhancer. This system involves 3 crosslinking pathways: two radical-mediated (or electron transfer) pathways (1 and 2), and one oxygen-mediated (or energy transfer) pathway (3). The ground state photosensitizer (PS), RB or RF, is excited to its triplet excited state T* by a quantum yield (q). In a type-I process, [T] interacts directly with [A] and [B] to form the first-radicals R and S, then produce the reactive intermediates R' and S' which could interact with oxygen [O_2], [A], [B], or bimolecular termination. For a type-II (or oxygen-mediated) process, [T] interacts with [O_2] to form a singlet oxygen [O_1] which could interact with [A], [B], or relaxed to [O_2].

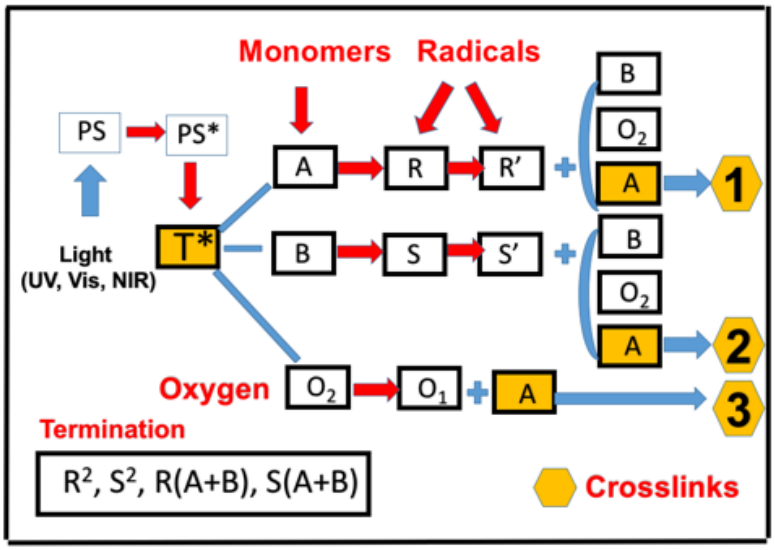

Fig. 1 Schematics of 3 photochemical pathways in a two-monomer system, A and B, in the presence of oxygen O_2, for radical-mediated pathways (1 and 2), and oxygen-mediated pathway (3); where PS is the ground state photosensitizer, having an excited and triplet state PS* and T*.

2.1 Photochemical Kinetics

The kinetic equations for a previous 1-monomer [A] system [6] are revised for a 2-monomer ([A] and [B]) system as follows (noting that [A] and [B] are symmetrically related); where short-hand notations for the concentrations are used: T for triplet state, [O_2] and X for oxygen ground and singlet state; R,R',S, S' for the radical concentrations;

$$\frac{\partial C(z,t)}{\partial t} = -bI(z,t)C - k_{11}XC + (k_5 + k_3[O_2])T + R_E \qquad (1.a)$$

$$\frac{\partial T}{\partial t} = bI(z,t)C - (k_5 + k_3[O_2] + k_{71}[A] + k_{72}[B])T \qquad (1.b)$$

$$\frac{\partial R}{\partial t} = k_{71}T[A] - k_{12}RR' - 2k_{t1}R^2 \quad (1.c)$$

$$\frac{\partial S}{\partial t} = k_{72}T[B] - k_{22}SS' - 2k_{t2}S^2 \quad (1.d)$$

$$\frac{\partial R\prime}{\partial t} = 2k_{t1}R^2 - k_{12}RR' - 2k_{t1}R'^2 - k_{91}R'[O_2] - G \quad (1.e)$$

$$\frac{\partial S\prime}{\partial t} = 2k_{t2}S^2 - k_{22}SS' - 2k_{t2}S'^2 - k_{92}S'[O_2] + G \quad (1.f)$$

$$\frac{\partial X}{\partial t} = k_3[O_2]T - (k_6 + k_{11}C + k_{81}[A] + k_{82}[B])X \quad (1.h)$$

$$\frac{\partial [O_2]}{\partial t} = P - k_3[O_2]T + k_6X - R_E \quad (1.i)$$

$$\frac{\partial [A]}{\partial t} = -(k_{71}[T] + k_{81}X + k_{41}R' + k_{51}S')[A] \quad (1.j)$$

$$\frac{\partial [B]}{\partial t} = -(k_{72}[T] + k_{82}X + k_{42}R' + k_{52}S')[B] \quad (1.k)$$

$$R_E = (k_{91}R' + k_{92}S')[O_2] \quad (1.l)$$

$$G = k_{42}R'[A] - k_{42}S'[B] \quad (1.m)$$

where b=83.6a'wq, with w being the UV light wavelength (in cm) and *q* is the triplet state [T] quantum yield, a' in (1/mM/%) and I(z,t) in mW/cm^2, b=0.62q, for UV light at 365 nm (with a'=204 (1/mM/%). For RGX with green light, the b value is approximately 4 time larger and having a smaller penetration depth of 100 um [8]. Eq. (1.i) also includes an oxygen source term given by $P=(1-X/X_0)\ P_0$, with a maximum rate constant P_0. All the reaction rate constants are defined by the associated coupling terms. For examples, in Eq. (1.b), k_{71} is for the reaction of [A] and T, which has a ground state relaxation rate k_5; in Eq. (1.c), k_{41} is for the reaction of [A] and R, which is coupled with R' by k_{12} and a bimolecular termination rate of k_{t1}; In Eq. (1.f), k_{42} is for the reaction of [A] and R', which is coupled with oxygen by k_{91} and a bimolecular termination rate of k_{t1}.

The dynamic light intensity is given by [3,4]

$$\frac{\partial I(z,t)}{\partial z} = -A'(z,t)I(z,t) \quad (2.a)$$

$$A'(z,t) = 2.3[(a' - b')C(z,t) + b'C_0F' + Q'] \quad (2.b)$$

a' and b' are the extinction coefficients of PS and the photolysis product, respectively; Q' is the absorption coefficient of the stroma at UV (365 nm) or green (532 nm) wavelength.

The kinetic equations (1) and (2) may be numerically calculated to find the CXL efficacy, which however is too complex for us to analyze the roles of each of the parameters. For comprehensive modeling we will use the so-called quasi-steady state assumption [2, 3] described as follows. The life time of triplet states of PS, the radicals (R and R'), and the singlet oxygen (X*) are very short (ns to μs time scale) since they either decay or react with cellular matrix immediately after they are created. Thus, one may set the time dependences, dT/dt=dX*/dt=dR/dt=dR'/dt=dS/dt=dS'/dt=0, or the so called quasi-steady-state conditions; defining $k_{91}= k_{92} =k$, $k_{81}= k_{82} =k_8$, $k_{71}= k_{72} =k_7$, $k_{41}= k_{42} = k_{51}= k_{52} =k'$, $k_{t1}= k_{t2} =k_T$; $k_{37}= k_3/k_7$, $k_{18} = k_8/k_{11}$, $k_{57}= k_5/k_7$, $k_{61}= k_6/k_{11}$, $T=bIgC$, $X=bIg'[O_2]K_{12}$, $g=1/(k_{37}[O_2]+[A]+ [B]+k_{57})$, $g'=k_{37}g$,

K_{11}= $k_{37}/(k_{61}+ k_{11}C+k_{18}[A]+k_{18}[B])$; $K_{22}= k_{37}[1-(k_6/k_{11})K_{11}]$, $K_{12}= (k_8/k_{11})K_{11}$, Eq. (2) becomes [4,5]

$$\frac{\partial C(z,t)}{\partial t} = -bIg([A] + [B] + K_{11}[O_2])C + R_E \quad (3.a)$$

$$\frac{\partial [O_2]}{\partial t} = -[bIgCK_{22} + k(R' + S')][O_2] + P \quad (3.b)$$

$$\frac{\partial [A]}{\partial t} = -[bIgC(1 + K_{12}[O_2]) + k'R_t]\,[A] \quad (3.c)$$

$$\frac{\partial [B]}{\partial t} = -[bIgC(1 + K_{12}[O_2]) + k'R_t]\,[B] \quad (3.c)$$

$$R_t = R' + S' \quad (3.e)$$

The radicals, R, R', S and R', are given by the solution of the following steady-state of Eq. (1.c) and (1.d): For $k_{12}R'<<2k_TR'$, $k_{22}S'<<2k_TS'$ Eq. (1.c) and (1.d) give steady-state $R=[bIgC[A]/k_T]^{0.5}$, and $S=[bIgC[B]/k_T]^{0.5}$. Using these R and S, we may find the steady-state solution of Eq. (1.e) and (1.f) given by

$$2k_{t1}R^2 - k_{42}R'[A] - k_{12}RR' - 2k_TR'^2 - kR'[O_2] = 0 \quad (4.a)$$

$$2k_{t2}S^2 - k_{52}S'[B] - k_{22}SS' - 2k_TS'^2 - kS'[O_2] = 0 \quad (4.b)$$

Eq. (40 has solution given by, for $kR'[O_2]>> k'R'[A]$, $k_{12}RR'$ in Eq. (4.a); and $kS'[O_2]>> k'R'[B]$, $k_{12}SS'$ in Eq. (4.b), R'=S' and both are given by

$$R'(z,t) = \left(\frac{1}{4\,k_T}\right)[-k[O_2] + \sqrt{(k\,[O_2])^2 + 8k_TB(z,t)}\ ] \quad (4.c)$$

where B=bIC, with approximated g[A]=g[B]=1.
For $(k[O_2])^2 <<8k_TB$, Eq. (4.c) is further reduced to $R'=(2B/k_T)^{0.5}- k[O_2](1-B')/(4k_T)$, with $B'= 0.5k[O_2]/(8Bk_T)^{0.5}$.

2.2 Conversion Efficacy

Numerical solutions are required for Eq. (4.a) and (4.b). However, analytic formulas are available for the following limiting cases. For $k_{41}R[A]$, $k_{51}S[B]$ and bIgC are the two dominant terms, For $k_{12}R'>>k_{42}[A]$, $k_{91}[O_2]$, $k_{22}S'>>k_{52}[B]$, Eq. (4) gives R'+S'=(1-d)(R+S), with $d=0.25k_{12}/k'$. Using these approximate solutions of R and R', Eq. (3) reduces to

$$\frac{\partial C(z,t)}{\partial t} = -bIg([A] + [B] + K_{11}[O_2])C + R_E \quad (5.a)$$

$$\frac{\partial [O_2]}{\partial t} = -bI(k_{37}gC + K_{22})[O_2] + P \quad (5.b)$$

$$\frac{\partial [A]}{\partial t} = -R_T[A] \quad (5.c)$$

$$\frac{\partial [B]}{\partial t} = -R_T[B] \quad (5.d)$$

$$R_T = bICg(1 + K_{12}[O_2]) + K_{13} \quad (5.e)$$

$$K_{13} = k'R\left[1 + \left(\frac{[B]}{[A]}\right)^{0.5}\right] - 0.5K_{23}[O_2] \qquad (5.f)$$

where K_{23}= k'k_9/k_T; R_E=(k_9K_{13}/k')[O_2]; and R=[0.5bIgC[A]/k_T]$^{0.5}$. Where we have defined a total rate function (R_T) for the monomer conversion consisting of three parts: the coupling of [A] with the triplet-state (the first term bIgC), the singlet oxygen (K_{12} term), and the radicals R' and S' (K_{13} term). Furthermore, K_{13} consists of the radical formation and the quenching effect due to oxygen (second term of Eq. (5.e).

The conversion efficacy of monomer [A] is defined by C_A=1- [A]/$[A]_0$ = 1- exp(-S), where the S function is given by the time integral of the total rate function, R_T, given by Eq. (5.e). For the type-I predominant case with [A]>>K_{11}[O_2], R_E, in Eq. (5.a), we have previously developed approximated analytic formulas for I(z,t) and C(z,t) [ ]

$$I(z,t) = I_0 \exp[-A'z] \qquad (6.a)$$

$$C'(z,t) = C_0 \exp[-B't] \qquad (6.b)$$

$$A'(\mathrm{z,t}) = 2.3(\mathrm{a'}C_0 + \mathrm{Q}) - A_1\mathrm{t} \qquad (6.c)$$

where B'=bI_0exp(-A"z), A_1=2.3(a'-b')C_0I_0bz, with A" is the averaged absorption given by A"=1.15(a'+b')+2.3Q. We note that the – A_1t term represents the decrease of A', or increase of light intensity due to the PS depletion.

Numerical solution of Eq. (5) will be shown later. Using Eq. (6), analytic solution of Eq. (5.c) and the S-function are available when K_{23}[O_2] is neglected and [B]<<[A], g[A]=1, as follows

$$\mathrm{S} = \mathrm{k'}G(z,t)\sqrt{0.5bXI_0C_0/k_T} \qquad (7.a)$$

$$\mathrm{G(z,t)} = [1 - \exp(-\mathrm{B"t})]/B" \qquad (7.b)$$

where B"=0.5(B'- A_1), X=exp[-A_2z], with A_2=1.15(a'+b')C_0+2.3Q. We note that Eq. (8) defines the dynamic feature of the light intensity which is an increasing function of time due to the depletion of the RF concentration. It also provides the nonlinear dynamic dependence of A'(z,t), given by A_1t, which is important for optical-thick polymer and for high light dose.

To discuss the role of the lifetimes of the triplet-state (T_1) and singlet-oxygen (T_2), Eq. (5) may be expressed by as follows:

$$\frac{\partial \mathrm{C(z,t)}}{\partial \mathrm{t}} = -\mathrm{bIC}\,[\,\mathrm{g([A]+[B])} + \mathrm{K}T_2[O_2]) + \mathrm{R_E} \qquad (8.a)$$

$$\frac{\partial \mathrm{[A]}}{\partial \mathrm{t}} = -\,\mathrm{bIgC}(1 + K'T_2[O_2])\mathrm{[A])} - \mathrm{k'(R' + S')[A]} \qquad (8.b)$$

$$\frac{\partial \mathrm{[B]}}{\partial \mathrm{t}} = -\,\mathrm{bIgC}(1 + K'T_2[O_2])\mathrm{[B]} - \mathrm{k'(R' + S')[B]} \qquad (8.c)$$

where g= k_7T_1, K= k_{11}(k_3/k_7), K'=k_8(k_3/k_7).

$$T_1 = 1/(k_5 + k_3[O_2] + k_7\mathrm{[A]} + k_7\mathrm{[B]}) \qquad (9.a)$$

$$T_2 = 1/(k_6 + k_{11}C + k_8\mathrm{[A]} + k_8\mathrm{[B]}) \qquad (9.b)$$

2.3 Crosslink depth (Z_C) and Crosslink time (T_C)

A crosslink depth (Z_C) and crosslink time (T_C) are defined by when the efficacy reaches a threshold value (C_T) at a depth t and z. Using Eq. (7), and let S= S_T=2 (or C_{EFF}=0.86), Z_C is related T_C by

$$T_C = \left(\frac{1}{B"}\right) \ln[2B"/(K'\sqrt{0.5bX'I_0C_0}) - 1] \qquad (10)$$

where K'= $k'/k_T^{0.5}$, X'=exp(-A"Z_C). Eq. (10) is a nonlinear equation of Z_C which can be numerically plot by rotating the curve of T_C vs Z_C to show the curve of Z_C vs T_C (to be shown later).

3. RESULTS AND DISCUSSION

Numerical results of Eq. (8) will be presented elsewhere, the following important features are available just based on Eq. (8) and (9) without solving them numerically.

Analysis of UVX and RGX

Eq. (5) defines the conversion rate (R_T) of monomers, which has three parts contributed by the the coupling of [A] or [B] with the triplet-state ([T]), the singlet oxygen [O-], and the radicals R' and S' (the K_{13} term). As shown by Eq. (5.e) and (6), R_T proportional to the lifetimes T_1 (for triplet state), and T_2 (for singlet-oxygen), oxygen concentration, [O_2], and the rate constants (kj). Base on Eq. (5) to (10), we are able to analyze the measured results of Wertheimer et al [7] as follows:

(a) For UVX system, with K_{CP}>>1, as proposed by Kamaev et al [8] Semchishen et al [9] and Lin [4,5] that CXL is predominated by type-I, which does not require oxygen, in contrast to Kling et al [12] proposing type-II oxygen=mediated system. The type-I conversion efficacy, given by C_A=1-exp(-S), with S is he time integral of R_T, and has a state-state value proportional to the $[C/(bI)]^{0.5}$, for a bimolecular termination process [5]. In this UVX system, the oxygen inhibition effect reduces the lifetime, as shown by Eq. (6.d) with T_1=g/k_7, which has a reduction factor (k_{57} + k_{37}[O_2])/([A]+[B]), and thus reduces the conversion efficacy. The oxygen inhibition effect also defines a so called "induction time" for the efficacy function, when oxygen is totally depleted, and thus type-I efficacy starts to increase faster.

(b) In contrast to UVX, RGX is predominated by an oxygen-mediated type-II process, where the single-monomer radical (R') induced type-I conversion is not very efficient. Therefore, additive enhancer-monomer was proposed by Wertheimer et al [7] for improved efficacy.

(c) For RGX with an additive enhancer (arginine), the conversion could be enhanced due to the extra radical term in Eq. (6), k'(R+S), in which the total rate function given by Eq. (5.e) has an enhance factor of $[1+((k_{72}/k_{71})\ [B]/[A])^{0.5}]$; which is proportional to the initial concentration ratio $[B_0]/[A_0]$, and their rate constant ratio, k_{72}/k_{71}. Therefore, in the absence of oxygen and without the enhancer [B] (or S=0), the conversion is contributed from $k_{71}T_1$ and k'R, which might not sufficient for effective crosslinking, which is enhanced by the extra monomer [B] and its radical S'. These features are measured by Wertheimer et al [7] that in an O_2-free environment, arginine was required for an increase in tensile strength.

(d) In the presence of deuterium oxide (D_2O), which extends the lifetime of singlet oxygen, i.e., a smaller relaxation rate (k_6), thus a larger T_2, based on our Eq. (7.b). In contrast, sodium azide which quenches singlet oxygen and other reactive radicals (R and S), i.e., increasing of k_5 and k_6, thus shortening T_1 and T_2, and partially inhibited RB photobleaching, shown by Eq. (6.a) with a reduced conversion as measured by Wertheimer et al [7]. This feature is also predicted by our quenching factors shown in Eq. (8), Q and Q', which reduce the lifetimes.

(e) As measured by Wertheimer et al [7], the increase in stiffness of corneas irradiated in air was not enhanced by arginine at low dose of 100 J/cm^2. This may be analyzed by our formula that the arginine-enhancement factor is proportional to $E_F=(btE_0k_{72}[B_0]/[A_0])^{0.5}$, with E_0 being the light dose, thus there is a threshold light dose (or intensity x time) and threshold arginine initial concentration $[B_0]$ to achieve stiffness increase in cornea.

(f) Our Z_C-formula, in Eq. (10) show that higher dose (E_0) is needed for a deeper Z_C. Thus, for a given depth, the enhanced dose factor (E_F) of arginine will reduce the required light dose (E_0). Our formula predicts the measured feature of Wertheimer et al[1] that RB staining solution contained arginine substantial photobleaching occurred at much lower fluence than in incisions without arginine. It also predicts that there is a threshold light dose and enhancement-threshold initial concentration of arginine.

(g) For RGX, type-II is predominant, as proposed by Wertheimer et al [7], whereas type-I is predominant in UVX [4,5,10,11]. This controversial issue of the role of oxygen in RF-system was explained by Wertheimer et al [7] that O_2 diffused deeper and crosslinking occurs at a greater depth in the tissue, after the crosslinkable sites was reacted. However, our formulas support the kinetic proposed by Kamaev et al [10] and Semchishen et al [11] that type-I and type-II co-exist, initially, and then predominated by type-I after oxygen is depleted.

(h) Eq. (5.e) and (5.f) show that Our formulas, Eq. (4.e) and (4.f) show that a system is type-I or type-II predominated depending on a ratio $R_A=K_{13}/(BK_{12}[O_2])$. When $R_A>0.8$, type-I is predominant, whereas type-II is predominant, for $R_A<0.2$ (or for large singlet-oxygen rate constant, $k_{37}k_8$). In general, both type-I and type-II co-exists initially (with R_A having a value of 0.5 to 1.5), until oxygen is depleted (or when $k_{37}k_8[O_2]=0$).

(i) Oxygen may play an enhancement or inhibition effect for the overall efficacy. This feature may be analyzed by the two-competing components shown by R_T in Eq. (5.e): the $K_{12}[O_2]$ term provides the oxygen-mediated type-II efficacy; whereas the reduction factor of g, $(k_3/k_7)[O_2]/[A]+[B]$ and second term of Eq. (4f), $0.5K_{23}[O_2]$, both cause oxygen inhibition. Therefore, the net effect of oxygen is the balance between these two components. The efficacy of type-II CXL may be enhanced by external oxygen diffusion, or under high oxygen pressure environment [12,15].

Greater details of the roles of oxygen in CXL [12-16], anticancer [17-18] and 3D bioprinting [19-20] have been reported. Numerical results of this study to investigate the role of oxygen, comparing to the clinical data of Wertheimer et al [7] will be published elsewhere.

4. CONCLUSION

Efficacy may be improved by additive enhancer-monomer in a 2-monomer system or extended lifetime of photosensitizer triplet-state or oxygen singlet. Our theory predicts the measured results.

CONSENT

It is not applicable.

ETHICAL APPROVAL

It is not applicable.

REFERENCES

1. Hafezi F and Randleman JB. editors. Corneal Collagen Cross-linking, second ed. Thorofare (NJ): SLACK; 2017.
2. Lin JT. Photochemical Kinetic modeling for oxygen-enhanced UV-light-activated corneal collagen crosslinking. Ophthalmology Research, 2017;7:1-8. DOI: 10.9734/or/2017/35032.
3. Lin JT. Efficacy S-formula and kinetics of oxygen-mediated (type-II) and non-oxygen-mediated (type-I) corneal cross-linking. Ophthalmology Research. 2018; 8:1-11, Article no.OR.39089. DOI : 10.9734/OR/2018/39089.
4. Lin JT, Cheng DC. Modeling the efficacy profiles of UV-light activated corneal collagen crosslinking. PloS One. 2017;12:e0175002. DOI:10.1371/journal.pone.0175002.
5. Lin JT. A proposed concentration-controlled new protocol for optimal corneal crosslinking efficacy in the anterior stroma. Invest. Ophthalmol Vis Sci. 2018;59:431–432.
6. Lin JT. Kinetics of Radicals-Oxygen Interaction and Enhanced efficacy for Corneal Cross-linking: Part-I (1-monomer system). Ophthalmology Research. 2019 (submitted).
7. Wertheimer CM, Elhardt C, Kaminsky SM et al. Enhancing rose Bengal photosensitized protein crosslinking in the cornea. Invest. Ophthalmol Vis Sci. 2019, 60, 1845-1852.
8. Zhu H, Alt C, Webb RH, Melki S, Kochevar IE. Corneal crosslinking with rose bengal and green light: efficacy and safety evaluation. Cornea. 2016;35:1234–1241.
9. Bekesi N, Gallego-Munoz P, Ibarea-Frias L, et al. Biomechanical Changes After In Vivo Collagen Cross- Linking With Rose Bengal–Green Light and Riboflavin-UVA Invest. Ophthalmol Vis Sci. 2017, 58, 1612-1620.
10. Kamaev P, Friedman MD, Sherr E, Muller D. Cornea photochemical kinetics of corneal cross-linking with riboflavin. Vis. Sci. 2012;53:2360-2367.
11. Semchishen A, Mrochen A, Semchishen V. Model for optimization of the UV-A/Riboflavin strengthening (cross-linking) of the cornea: percolation threshold. Photochemistry and photobiology, 2015; 91:1403-1411.
12. Kling S, Hafezi F. An algorithm to predict the biomechanical stiffening effect in corneal cross-linking. J Refract Surg 2017; 32:128-136. doi:10.3928/1081597X-20161206-01.
13. Kling S, Richoz O, Hammer A, et al. Increased biomechanical efficacy of corneal cross-linking in thin corneas due to higher oxygen availability. *J Refract Surg.* 2015;31:840-846.
14. Huang R, Choe E, Min DB. Kinetics for singlet oxygen formation by riboflavin photosensitization and the reaction between riboflavin and singlet oxygen. *J Food Sci.* 2004;69:C726-C732.
15. Larrea X, Büchler P. A transient diffusion model of the cornea for the assessment of oxygen diffusivity and consumption. *In- vest Ophthalmol Vis Sci.* 2009;50:1076-1080.
16. Richoz O, Hammer A, Tabibian D, Gatzioufas Z, Hafezi F. The biomechanical effect of corneal collagen cross-linking (CXL) with riboflavin and UV-A is oxygen dependent. *Transl Vis Sci Technol.* 2013;2:6.
17. Zhu TC, Finlay JC, Zhou X, et al. Macroscopic Modeling of the singlet oxygen production during PDT. Proc SPIE. 2007; 6427:6427O81–6427O812.
18. Wang KKH, Finlay JC, Busch TM, et al. Explicit dosimetry for photodynamic therapy: macroscopic singlet oxygen modeling. Journal of Biophotonics. 2010; 3(5-6):304–318. [PubMed: 20222102].
19. de Beer, M. P.; van der Laan, H. L.; Cole, M. A.; Whelan, R. J.; Burns, M. A.; Scott, T. F. Rapid, Continuous Additive Manufacturing by Volumetric Polymerization Inhibition Patterning. Sci. Adv. 2019, 5, 8.
20. Zhu W, Tringale KR, Woller SA, et al. Rapid Continuous 3D Printing of Customizable Peripheral Nerve Guidance Conduits. Mater. Today 2018, 21, 951–959.